First integrals for the Kepler problem with linear drag

Alessandro Margheri[*]

Fac. Ciências da Univ. de Lisboa e

Centro de Matemática, Aplicações Fundamentais e Investigação Operacional,

Campo Grande, Edifício C6, piso 2, P-1749-016 Lisboa Portugal

e-mail: amargheri@fc.ul.pt

Rafael Ortega[†]

Departamento de Matemática Aplicada,

Universidad de Granada, 18071 Granada, Spain

e-mail: rortega@ugr.es

Carlota Rebelo[‡]

Fac. Ciências da Univ. Lisboa e

Centro de Matemática, Aplicações Fundamentais e Investigação Operacional,

Campo Grande, Edifício C6, piso 2, P-1749-016 Lisboa Portugal

e-mail: mcgoncalves@fc.ul.pt

July 4, 2016

Abstract

In this work we consider the Kepler problem with linear drag, and prove the existence of a continuous vector-valued first integral, obtained taking the limit as $t \to +\infty$ of the Runge-Lenz vector. The

[*]Supported by Fundação para a Ciência e Tecnologia, UID/MAT/04561/2013

[†]Supported by project MTM2014-52232-P, Spain.

[‡]Supported by Fundação para a Ciência e Tecnologia, UID/MAT/04561/2013

norm of this first integral can be interpreted as an asymptotic eccentricity e_∞ with $0 \leq e_\infty \leq 1$. The orbits satisfying $e_\infty < 1$ approach the singularity by an elliptic spiral and the corresponding solutions $x(t) = r(t)e^{i\theta(t)}$ have a norm $r(t)$ that goes to zero like a negative exponential and an argument $\theta(t)$ that goes to infinity like a positive exponential. In particular, the difference between consecutive times of passage through the pericenter, say $T_{n+1} - T_n$, goes to zero as $\frac{1}{n}$.

Keywords: Kepler equation, linear drag, first integral, conformally symplectic

1 Introduction

In this work we prove the existence of a Runge-Lenz-type first integral for the Kepler problem with linear drag,

$$\ddot{x} + \epsilon\dot{x} = -\frac{x}{|x|^3}, \quad x \in \mathbb{R}^2 \setminus \{0\}, \tag{1}$$

where the dot denotes the derivative with respect to time and ϵ is a positive constant. Using this first integral we can give a geometrical description of the evolution of the orbits, as well as quantitative estimates of the corresponding solutions. These results, together with those in [14], allow to give a fairly complete characterization, mostly from a qualitative point of view, of the global dynamics associated to equation (1).

Our approach is based on the ideas on asymptotic integrals developed by Moser in [16] for the study of the Störmer problem (see also [17]). Given a solution $x(t)$ of (1) with $x(0) = x_0$ and $\dot{x}(0) = v_0$, we will consider the corresponding Runge-Lenz vector $R(t)$ and prove that the limit

$$I = \lim_{t \to +\infty} R(t)$$

exists. Just from the definition it follows that the vector $I = I(x_0, v_0)$ is a constant of motion. As we will see this vector contains relevant information on the orbit.

Runge-Lenz-type vectors (also referred to as Hamilton-like vectors or as Laplace-like vectors) have been already used in the literature on dissipative problems (see [13], [11], [15]). These vectors are useful to deduce the orbit equation in a Kepler problem with the so called Poynting-Plummer-Danby drag (see [7] and [3] and the references therein). In this case the corresponding equation is of the form

$$\ddot{x} + D(x, \dot{x})\dot{x} = -\frac{x}{|x|^3}, \quad x \in \mathbb{R}^2 \setminus \{0\}, \tag{2}$$

with

$$D(x,\dot{x}) = \frac{\alpha}{|x|^2}, \tag{3}$$

and $\alpha > 0$. In general, in these works, taking advantage of the integrability of equation (2) with dissipation (3), a closed form formula involving the Runge-Lenz vector is provided for the orbit equation, that is given as a function of the polar angle. Some corresponding numerical simulations are presented to show how the orbits spiral down towards the singularity.

Our interest in the linear dissipation is mainly driven by the attempt to give a contribution to a qualitative theory of the dissipative Kepler problem. Ideally, one would like to be able to divide the drags in classes according to the global dynamics they induce in the phase space. In this setting, as far as we know, there are few results. In [6] a dissipative force such that

$$D(x,\dot{x}) = k(|\dot{x}|)/|\dot{x}| \tag{4}$$

is considered. Assuming the convergence of a suitable integral, it is shown that all solutions go to the singularity (but it is not studied if that occurs in finite or infinite time). In particular the assumption holds when $k(|\dot{x}|) = \epsilon|\dot{x}|^\alpha,\ \epsilon > 0$ (a drag introduced by Jacobi in [12]) and $\alpha < 1$. We point out that the linear drag is a particular case of the Jacobi's drag.

From our perspective, it is very interesting the fairly exhaustive qualitative study presented in [8] for the Kepler problem with a generalized Stokes's drag force of the type

$$F(x,\dot{x}) = \frac{\alpha \mathbf{v}_r + \beta \mathbf{v}_\theta}{|x|^2}, \tag{5}$$

where α and β are positive constants and $\mathbf{v}_r$, $\mathbf{v}_\theta$ are, respectively, the radial and angular vector components of the velocity. It is worth to recall that the important Poynting-Robertson drag is a special case of (5). The same problem was already considered in [3] from an analytical point of view. Comparing our results with the ones in [8], we see that the way many solutions approach the singularity in the Kepler problem with drag (5) is sharply different from the one corresponding to the solutions of equation (1). Postponing to Section 4 the discussion on this point, we focus here on the results we have obtained for the solutions of (1). In [14] we showed that the non linear motions of (1) approach the singularity in infinite time. In this work, exploiting the existence of the aforementioned first integral, we prove that, actually, as t goes to $+\infty$ the orbits with $|I| < 1$ are asymptotically of the form $y(t)e^{-2\epsilon t}$, where $y(t)$ travels along a suitable fixed ellipse (see Corollary 3.1) with an angular velocity that grows exponentially with t (see Corollary 3.3). As a consequence, the orbits pass infinite times through the pericenter

and the time T_n of the n-th passage behaves like $\frac{1}{3\epsilon}\log n$ for n large. In addition, the time between two consecutive passages through the pericenter tends to zero as $\frac{1}{n}$. This last property is reminiscent of the phenomenon of decreasing orbital periods observed from the data of the orbital parameters collected from the Sputnik 1 mission [18, page 105]. As it is well known, the atmospheric drag effects are of non linear type (see [2]). We think that some theoretical work on non linear drags is needed to understand some observed aspects of the dynamics of the corresponding Kepler problem (see Section 4 for more details).

Qualitative results for a Kepler problem with dissipation are also obtained in [1], where a simple model to study the effect of tidal dissipation on the motion of celestial bodies is presented. For the general class of dissipative forces considered to model the tidal effect, it is found that every non rectilinear orbit approaches a circular orbit with nonzero angular momentum.

A linear dissipation term has already been considered in celestial mechanics to model the so-called 'spin-orbit problem' (see, for example, [4]) leading to the study of conformally symplectic systems [5]. In this connection, it may be worth to point out that among all the dissipative mechanisms corresponding to equations of the form $\dot{x} = y,\ \dot{y} = -D(x,y)y - \nabla V(x),$ the linear one (with $D(x,y) = \textit{positive constant}$) is the unique to generate a flow that is a conformally symplectic mapping.

This paper is organized as follows. In Section 2 we prove the existence of the first integral and discuss some of its properties. In Section 3 we use the first integral to get geometrical informations about the orbits as well as some estimates on the asymptotic dynamics of non rectilinear motions of (1). Also, we single out two open subsets of the phase space whose intersection corresponds to solutions of (1) on which the first integral I satisfies $0 < |I| < 1$. For one of these solutions we present a simulation to illustrate our results. Section 4 contains a discussion of our results. Finally, in the Appendix we give the proof of an auxiliary result, namely Lemma 2.2.

2 Existence of the Runge-Lenz-type first integral for the Kepler problem with linear drag

As mentioned in the previous section, the Kepler problem with linear drag is described by equation (1).

We consider the equivalent system in the phase space $\Omega = (\mathbb{R}^2 \setminus \{0\}) \times \mathbb{R}^2$

$$\begin{cases} \dot{x} = v \\ \dot{v} + \epsilon v = -\frac{x}{|x|^3}. \end{cases} \tag{6}$$

We recall that a solution of (1) (and hence of (6)) such that $x(0) = x_0$ and $\dot{x}(0) = v_0$ is defined for $t \in [0, \omega[$ where $\omega = \omega(x_0, v_0)$ is finite in the case of a rectilinear motion, whereas $\omega = +\infty$ for a non rectilinear motion. In any case, all solutions of (1) tend to the singularity, and are therefore bounded on $[0, \omega[$. The non rectilinear motions are actually defined for all time, come from infinity with energy which goes to $+\infty$ as $t \to -\infty$ and tend to the singularity with energy that goes to $-\infty$ (see [14] for more details).

In what follows, sometimes we will employ the notation $x(t; x_0, v_0)$ for the solution of (1) such that $x(0) = x_0$, $v(0) = v_0$, with $(x_0, v_0) \in \Omega$.

The conservative Kepler problem, which corresponds to $\epsilon = 0$, has many first integrals, but the most popular are the energy

$$E(x, v) = \frac{1}{2}|v|^2 - \frac{1}{|x|}, \tag{7}$$

the angular momentum[1]

$$C(x, v) = x \wedge v, \tag{8}$$

and the Runge-Lenz vector

$$R(x, v) = v \wedge (x \wedge v) - \frac{x}{|x|}. \tag{9}$$

None of the above quantities is preserved by the dissipative flow but we will show below in our main result that the Runge-Lenz vector has an analogue in system (6).

Theorem 2.1 *There exists a continuous vector field*

$$I : \Omega \to \mathbb{R}^2, \;\; I = I(x, v)$$

satisfying

(i) $I(\sigma x, \sigma v) = \sigma I(x, v)$, *for each* $(x, v) \in \Omega$ *and each rotation*

$$\sigma = \begin{pmatrix} \cos\theta & -\sin\theta \\ \sin\theta & \cos\theta \end{pmatrix}.$$

[1]From now on the wedge $\wedge$ will be employed to denote the vector product in $\mathbb{R}^3$. Due to the identification of $\mathbb{R}^2$ with $\mathbb{R}^2 \times \{0\} \subset \mathbb{R}^3$, the arguments of the vector product of the form $(w, 0) \in \mathbb{R}^3$ will be denoted simply by $w \in \mathbb{R}^2$.

(ii) The norm of I satisfies

$$|I(x,v)| \leq 1,\ (x,v) \in \Omega. \tag{10}$$

Moreover the function $e_\infty(x,v) := |I(x,v)|$ takes all values in the interval $]0,1]$.

(iii) Each solution $(x(t),v(t))$ of (6), defined on a maximal interval of the form $]\alpha,\omega[$, satisfies

$$I(x(t),v(t)) = \lim_{\tau\to\omega} R(x(\tau),v(\tau)). \tag{11}$$

Remark 1 The property (iii) implies that the coordinates of $I = (I_1, I_2)$ are first integrals of (6), that is $I(x(t),v(t)) =$ constant, for each solution $(x(t),v(t))$. By now we can only say that I is continuous, but it could be interesting to know if it has some additional smoothness properties. The properties (i) and (ii) imply that the two first integrals I_1 and I_2 are functionally independent. To see this, assume that $F : \mathbb{R}^2 \to \mathbb{R}$, $F = F(\xi_1,\xi_2)$ is a continuous function such that $F(I_1(x,v), I_2(x,v)) = 0$ for each $(x,v) \in \Omega$. Then F should vanish on the whole unit disk because the image of I is dense in this disk.

Remark 2 The invariance under rotations described in property (i) is also shared by the Runge-Lenz vector R. However the property (ii) has no analogue for R. In the conservative Kepler problem the condition $|R| > 1$ corresponds to hyperbolic motions. The condition $|I| \leq 1$ somehow expresses that there are no hyperbolic motions in the dissipative problem. This vague statement will become more precise after we discuss the geometric meaning of the theorem. Indeed if $\epsilon = 0$ and $|R| < 1$, the vector R is the eccentricity vector corresponding to the Keplerian ellipses. In particular, if $R \neq 0$, the unit vector $\dfrac{R}{|R|}$ is the direction of the major axis and $e = |R|$ is the eccentricity. In the dissipative case I can be interpreted as an asymptotic eccentricity vector and so e_∞ is an asymptotic eccentricity. Solutions with $|I| < 1$ tend to the origin along a spiral determined asymptotically by I. The geometry of the corresponding orbits will be described in Corollary 3.1.

In preparation for the proof of the theorem, we start by recalling two formulas, the first connecting the functions R and C, and the second linking the functions R, C and E, see also [10], 3-9, where these formulas are derived along the solutions of the Kepler problem. Here we stress the fact that they hold as functional relationship between functions of the real variables (x,v).

Namely, denoting by $< v, w >$ the inner product between the vectors v and w, we have

$$|x| + < R, x >= |C|^2, \text{ for any } x \in \mathbb{R}^2 \setminus \{0\} \tag{12}$$

and

$$|R|^2 - 1 = 2|C|^2 E. \tag{13}$$

The identity (12) follows from the properties connecting the inner and vector products. Indeed

$$\begin{aligned} |x| + < R, x > &= < v \wedge (x \wedge v), x >= - < (x \wedge v) \wedge v, x >= & (14) \\ &= - < x \wedge v, v \wedge x >= |x \wedge v|^2. & (15) \end{aligned}$$

To prove (13) we first observe that $v \perp x \wedge v$, and by (9) it follows that

$$\left| R + \frac{x}{|x|} \right|^2 = |v \wedge (x \wedge v)|^2 = |v|^2 |x \wedge v|^2. \tag{16}$$

Expanding the square we obtain

$$|R|^2 + 1 + \frac{2}{|x|} < R, x >= |v|^2 |C|^2. \tag{17}$$

Using (12) we get

$$|R|^2 + 1 + \frac{2}{|x|}(|C|^2 - |x|) = |v|^2 |C|^2 \tag{18}$$

and finally

$$|R|^2 - 1 = 2|C|^2 \left(\frac{1}{2}|v|^2 - \frac{1}{|x|} \right). \tag{19}$$

To end our preparatory work, we state the following lemma, needed to prove the continuity of I on Ω. Its proof is postponed to the Appendix.

Lemma 2.2 *Let K be a compact subset of Ω. Then there exists $m_K > 0$ such that*

$$|x(t; x_0, v_0)| \leq m_K$$

for any $(x_0, v_0) \in K$ and $t \in [0, \omega[$.

We are now in a position to prove our theorem.

Proof of Theorem 2.1 Fixed $(x_0, v_0) \in \Omega$, let $(x(t), v(t))$ be the solution of system (6) such that $(x(0), v(0)) = (x_0, v_0)$. In what follows we let $C(t) =$

$C(x(t), v(t))$ and denote by $\dot{C}$ its derivative with respect to time. Analogous notations will be used for R and E. For any smooth function $x = x(t)$,

$$\frac{d}{dt}\left(\frac{x}{|x|}\right) = \frac{1}{|x|^3}[(x \wedge \dot{x}) \wedge x] = C \wedge \left(\frac{x}{|x|^3}\right). \tag{20}$$

Hence, recalling that for the linear drag we have $\dot{C} = -\epsilon C$, along a solution of (6) we obtain

$$\begin{aligned} \dot{R} &= \ddot{x} \wedge C + \dot{x} \wedge \dot{C} - C \wedge \frac{x}{|x|^3} = \\ &= -\epsilon\, \dot{x} \wedge C - \frac{x}{|x|^3} \wedge C + \dot{x} \wedge \dot{C} - C \wedge \frac{x}{|x|^3} = \\ &= -2\epsilon\, \dot{x} \wedge C. \end{aligned}$$

From this identity it is easy to deduce the existence of the limit of R at $t = \omega$. In fact, as

$$R(t) = R(0) - 2\epsilon \int_0^t \dot{x}(\tau) \wedge C(\tau) d\tau \tag{21}$$

and $C(t) = C(0)\mathrm{e}^{-\epsilon t}$ we obtain

$$\begin{aligned} R(t) &= R(0) - 2\epsilon \int_0^t \mathrm{e}^{-\epsilon\tau}(\dot{x}(\tau) \wedge C(0)) d\tau \\ &= R(0) - 2\epsilon[\mathrm{e}^{-\epsilon\tau} x(\tau) \wedge C(0)]_0^t - 2\epsilon^2 \int_0^t \mathrm{e}^{-\epsilon\tau}(x(\tau) \wedge C(0)) d\tau. \end{aligned}$$

Now from the attraction of the origin, $x(t) \to 0$ as $t \to \omega$, we get

$$\lim_{t\to\omega} R(t) = R(0) + 2\epsilon\, x(0) \wedge C(0) - 2\epsilon^2 \int_0^\omega \mathrm{e}^{-\epsilon\tau}(x(\tau) \wedge C(0)) d\tau. \tag{22}$$

At this point we can define the function

$$I(x_0, v_0) = R(x_0, v_0) + 2\epsilon\, x_0 \wedge C(x_0, v_0) - 2\epsilon^2 \int_0^\omega \mathrm{e}^{-\epsilon\tau}(x(\tau; x_0, v_0) \wedge C(x_0, v_0)) d\tau. \tag{23}$$

To prove that I is a continuous function on Ω we use the standard results on functions defined by parametric integrals together with Lemma 2.2.

Since properties (i) and (iii) follow immediately from the definition of I, we prove now (ii). In the case $x_0 \wedge v_0 = 0$, by (23) we get $I(x_0, v_0) = R(x_0, v_0) = -\dfrac{x_0}{|x_0|}$ and therefore we have $|I(x_0, v_0)| = 1$. Let us assume then that $x_0 \wedge v_0 \neq 0$. Since $C(t) \neq 0$ everywhere and $E(t) \to -\infty$ when $t \to +\infty$,

by (13) we see that $|R(t)|^2 - 1 < 0$ if t is large enough. We conclude that $\lim_{t\to+\infty} |R(t)| \leq 1$ and hence

$$|I(x_0, v_0)| \leq 1. \tag{24}$$

Incidentally we notice that, since $|C(t)| \to +\infty$ and $E(t) \to +\infty$ as $t \to -\infty$ (see [14]), by (13) we get

$$\lim_{t\to-\infty} |R(t)| = +\infty. \tag{25}$$

Let us now analyse the range of $e_\infty = |I|$. We are going to work with initial conditions (x_0, v_0) satisfying $x_0 \wedge v_0 \neq 0$ and $E(x_0, v_0) < 0$. Then, as $v_0 \neq 0$,

$$|E(x_0, v_0)| = \frac{1}{|x_0|} - \frac{1}{2}|v_0|^2 < \frac{1}{|x_0|}. \tag{26}$$

Since $E(t)$ is decreasing

$$|x(t)| < \frac{1}{|E(t)|} \leq \frac{1}{|E(x_0, v_0)|}, \text{ if } t \geq 0. \tag{27}$$

From (23) we have

$$|I(x_0, v_0) - R(x_0, v_0)| < 4\epsilon \frac{|C(x_0, v_0)|}{|E(x_0, v_0)|}. \tag{28}$$

Let us apply this estimate to the sequence of initial conditions $x_0^{(n)} = (\frac{1}{n^2}, 0)$, $v_0^{(n)} = (0, n)$. Then $E(x_0^{(n)}, v_0^{(n)}) = -\frac{n^2}{2} < 0$, $|C(x_0^{(n)}, v_0^{(n)})| = \frac{1}{n} \neq 0$ and $R(x_0^{(n)}, v_0^{(n)}) = 0$. Then (28) implies that $|I(x_0^{(n)}, v_0^{(n)})| < \frac{8\epsilon}{n^3} \to 0$. Since we know that $|I| = 1$ if $x_0 \wedge v_0 = 0$ we deduce that $e_\infty = |I|$ takes all values on $]0, 1]$.

■

3 Geometrical and dynamical properties of the solutions

In this section we consider some consequences of Theorem 2.1. We present them in the three corollaries below. The first one deals with the geometry of the orbits for which $|I| < 1$, whereas the others give information on the way such orbits are traversed.

Let us recall that the family of ellipses with a focus at the origin is determined by the equation in $\mathbb{R}^2$

$$|x| + < L, x >= K^2, \tag{29}$$

where $L \in \mathbb{R}^2$, $|L| < 1$ and $K > 0$. From now on we denote by $\mathcal{E} = \mathcal{E}(L, K)$. the ellipse of this family corresponding to a fixed pair (L, K).

Corollary 3.1 *Fixed $(x_0, v_0) \in \Omega$, let $(x(t), v(t))$ be the solution of (6) such that $(x(0), v(0)) = (x_0, v_0)$. If*

$$|I(x_0, v_0)| < 1$$

then $\omega = +\infty$ and

$$e^{2\epsilon t} x(t) \to \mathcal{E} \text{ as } t \to +\infty, \tag{30}$$

where $\mathcal{E} = \mathcal{E}(L, K)$ with $L = I(x_0, v_0)$ and $K = |C(x_0, v_0)|$.

Proof. Since we know that for linear motions $|I(x_0, v_0)| = 1$, the condition $|I(x_0, v_0)| < 1$ implies that the corresponding motion is non rectilinear, so that $\omega = +\infty$ (see [14]). From (12) we conclude that

$$|\mathrm{e}^{2\epsilon t}\, x(t)| + < R(t), \mathrm{e}^{2\epsilon t}\, x(t) >= |C(x_0, v_0)|^2, \tag{31}$$

which means that, for each t, $\mathrm{e}^{2\epsilon t}\, x(t)$ belongs to an ellipse $\mathcal{E}$ of the form $\mathcal{E} = \mathcal{E}(I(x_0, v_0) + \phi(t), |C(x_0, v_0)|)$ where $\phi(t) \to 0$ as $t \to +\infty$.

■

As a consequence of the previous result, we are able to give some estimates about the asymptotic dynamical behaviour of the solutions.

Corollary 3.2 *Assume that $(x(t), v(t))$ is a solution of (6) satisfying*

$$|I(x_0, v_0)| < 1. \tag{32}$$

Then, the following estimates hold for sufficiently large t :

$$A_1 e^{-2\epsilon t} \leq |x(t)| \leq A_2 e^{-2\epsilon t} \tag{33}$$

$$B_1 e^{\epsilon t} \leq |\dot{x}(t)| \leq B_2 e^{\epsilon t} \tag{34}$$

for suitable constants $A_i > 0, B_i > 0,\ \ i = 1, 2.$

Proof. Let y_{min} and y_{max} denote, respectively, the distance from O at the pericenter and apocenter along the ellipse $\mathcal{E}(I(x_0, v_0), |C(x_0, v_0)|)$. From Corollary 3.1 we have that for each $\eta > 0$ there exists t_η such that for each $t \geq t_\eta$ we have

$$(y_{min} - \eta)\mathrm{e}^{-2\epsilon t} < |x(t)| < (y_{max} + \eta)\mathrm{e}^{-2\epsilon t} \tag{35}$$

and (33) is proved. Now, from (17) we obtain

$$(1 - |R|)^2 \leq |v|^2|C|^2 \leq (1 + |R|)^2 \tag{36}$$

and this implies that, choosing $\eta < 1 - |I|$ and if necessary a larger t_η,

$$\frac{(1 - |I(x_0, v_0)| - \eta)^2}{|C(x_0, v_0)|^2}\mathrm{e}^{2\epsilon t} \leq |\dot{x}(t)|^2 \leq \frac{(1 + |I(x_0, v_0)| + \eta)^2}{|C(x_0, v_0)|^2}\mathrm{e}^{2\epsilon t}, \tag{37}$$

for each $t \geq t_\eta$, and also (34) is proved.

■

Finally we give a result which describes quantitatively the way the solutions rotate around the origin as they spiral down to the singularity. Given a solution in the conditions of Corollary 3.1, the angular momentum does not vanish and so the orbit will rotate around the origin with positive or negative orientation. At least for sufficiently large time it makes sense to define the time of passage through the pericenter as a time T such that the solution crosses the ray spanned by the vector $I(x_0, v_0)$; that is,

$$x(T) = \lambda I(x_0, v_0) \tag{38}$$

for some $\lambda > 0$. If $I(x_0, v_0) = 0$ one can consider the intersection of the trajectory with any fixed ray emanating from the origin.

Corollary 3.3 *Assume that $(x(t), v(t))$ is a solution of* (6) *satisfying* (32). *Then the set of times $T \geq 2\pi$ defined by the condition* (38) *can be arranged in an increasing sequence $\{T_n\}_{n\geq 1}$ satisfying*

$$|T_n - \frac{1}{3\epsilon}\log n| \leq K_1 \tag{39}$$

$$\frac{K_2}{n} \leq T_{n+1} - T_n \leq \frac{K_3}{n} \tag{40}$$

where K_1, K_2 and K_3 are suitable positive constants.

As a consequence, the solution crosses infinitely many times the asymptotic eccentricity axis determined by $I(x_0, v_0)$. From the proof we will see that this solution winds around the origin faster and faster. Also we will obtain the estimates on the argument function that were announced in the abstract.

Proof. For the angular coordinate, defined by $x(t) = r(t)\mathrm{e}^{i\theta(t)}$, we have that

$$r^2(t)|\dot{\theta}(t)| = |C(x_0, v_0)|\mathrm{e}^{-\epsilon t}. \tag{41}$$

As $r(t) = |x(t)|$, by (35), we conclude that, for large t,

$$\frac{|C(x_0, v_0)|}{A_2^2}\mathrm{e}^{3\epsilon t} \leq |\dot{\theta}(t)| \leq \frac{|C(x_0, v_0)|}{A_1^2}\mathrm{e}^{3\epsilon t}. \tag{42}$$

This leads to the estimate

$$C_1\mathrm{e}^{3\epsilon t} \leq |\dot{\theta}(t)| \leq C_2\mathrm{e}^{3\epsilon t}, \;\; t \geq 0 \tag{43}$$

where $C_1 < \frac{|C(x_0,v_0)|}{A_2^2}$ and $C_2 > \frac{|C(x_0,v_0)|}{A_1^2}$ are suitable positive constants. Assuming for simplicity $\dot{\theta}(t) > 0$ (the case $\dot{\theta}(t) < 0$ is analogous) and $\theta(0) \in [0, 2\pi[$, we integrate (43) to get the inequality

$$D_1\mathrm{e}^{3\epsilon t} \leq \theta(t) \leq D_2\mathrm{e}^{3\epsilon t}, \;\; t \geq 0 \tag{44}$$

where $D_i > 0$, $i = 1, 2$, are suitable constants. Let $\theta_0 \in [0, 2\pi[$ be the argument of $I(x_0, v_0)$. The condition (38) is equivalent to $\theta(T) - \theta_0 \in 2\pi\mathbb{Z}$. Hence we can use (43) to deduce that, for each $n \geq 1$, the equation

$$\theta(T) = \theta_0 + 2n\pi \tag{45}$$

has a unique solution T_n. Moreover the sequence $\{T_n\}$ is increasing and tends to infinity. To prove (39) we evaluate (44) at $t = T_n$. To prove (40) we apply the intermediate value theorem to find $\xi_n \in]T_n, T_{n+1}[$ such that

$$2\pi = \theta(T_{n+1}) - \theta(T_n) = \dot{\theta}(\xi_n)(T_{n+1} - T_n). \tag{46}$$

Thus

$$C_1 e^{3\epsilon T_n}(T_{n+1} - T_n) \leq 2\pi \leq C_2 e^{3\epsilon T_{n+1}}(T_{n+1} - T_n) \tag{47}$$

and the estimate follows by a combination of these inequalities and (39). ∎

We do not know if there are motions with $|I| = 1$ and $C \neq 0$. If they exist they could be called asymptotically linear motions. The same is open for $I =$

0, corresponding to asymptotically circular motions. Our final proposition singles out two subsets Ω_1 and Ω_2 of the phase space which correspond to initial conditions of solutions of (1) for which, respectively, $0 < |I(x_0, v_0)|$ and $|I(x_0, v_0)| < 1$.

Proposition 3.4 *Let*

$$\Omega_1 = \left\{ (x,v) \in (\mathbb{R}^2 \setminus \{0\}) \times \mathbb{R}^2 \ : \ E(x,v) < 0, \ \frac{2\sqrt{2}\epsilon}{\sqrt{8\epsilon^2 + |E(x,v)|^3}} \leq |R(x,v)| \right\} \tag{48}$$

and

$$\Omega_2 = \left\{ (x,v) \in (\mathbb{R}^2 \setminus \{0\}) \times \mathbb{R}^2 \ : \ E(x,v) < 0, \ |R(x,v)| \leq \frac{|E(x,v)|^3 - 8\epsilon^2}{|E(x,v)|^3 + 8\epsilon^2} \right\}. \tag{49}$$

If $(x_0, v_0) \in \Omega_1$, *then* $|I(x_0, v_0)| > 0$. *If* $(x_0, v_0) \in \Omega_2$, *then* $|I(x_0, v_0)| < 1$.

Proof. Assume by contradiction that $(x_0, v_0) \in \Omega_1$ and that $I(x_0, v_0) = 0$. Then, by (28)

$$|R(x_0, v_0)| < 4\epsilon \frac{|C(x_0, v_0)|}{|E(x_0, v_0|}. \tag{50}$$

Squaring this inequality, and using it in (13) one gets readily

$$|R(x_0, v_0)| < \frac{2\sqrt{2}\epsilon}{\sqrt{8\epsilon^2 + |E(x,v)|^3}}, \tag{51}$$

which is absurd since $(x_0, v_0) \in \Omega_1$. The case $(x_0, v_0) \in \Omega_2$ is similar. ∎

Figures 1 and 2 below illustrate the geometrical content of Corollary 3.1 by considering a solution of (1) whose initial condition belongs to $\Omega_1 \cap \Omega_2$. For the same solution, the exponential growth of the polar angle stated in Corollary 3.3 is plotted in Figure 3. All the figures were obtained by using the MATLAB solver ode23 to numerically integrate equation (1).

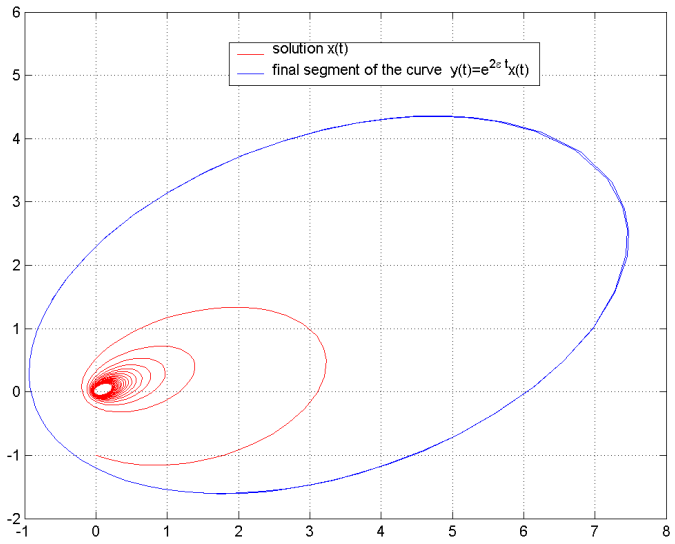

Figure 1: Plots of a solution $x(t),\ t \in [0, 35]$, of (1) with $\epsilon = 0.01$ and initial condition $(x_0, v_0) = (0, -1, \sqrt{3}/2, -1/2) \in \Omega_1 \cap \Omega_2$, and of the corresponding curve $y(t) = e^{2\epsilon t}x(t)$ which approximates the ellipse $\mathcal{E}$ defined in Corollary 3.1. To have a better view of the approximate shape of $\mathcal{E}$ only the final segment of the curve $y(t) = e^{2\epsilon t}x(t)$ was plotted.

4 Discussion

In this work we showed that the Kepler equation with linear drag admits a continuous vector-valued first integral and we exploited it to obtain both geometrical and dynamical insights about the non rectilinear orbits and the corresponding solutions. These results complement those in [14] and allow to understand thoroughly the global dynamics of (1), making possible a comparison with the dynamics produced by other drags. However, due to the lack of available qualitative results, we were able to carry out a detailed comparison just with the generalized Stokes's drag force

$$F(x, \dot{x}) = \frac{\alpha \mathbf{v}_r + \beta \mathbf{v}_\theta}{|x|^2}, \quad \alpha,\ \beta > 0. \tag{52}$$

As showed in [8], for this resistive force many non rectilinear solutions, corresponding to an open set of initial conditions, collide in finite time and with finite velocity with the singularity, spiralling just a finite number of times before collision. Moreover, the approach to the singularity occurs with angular

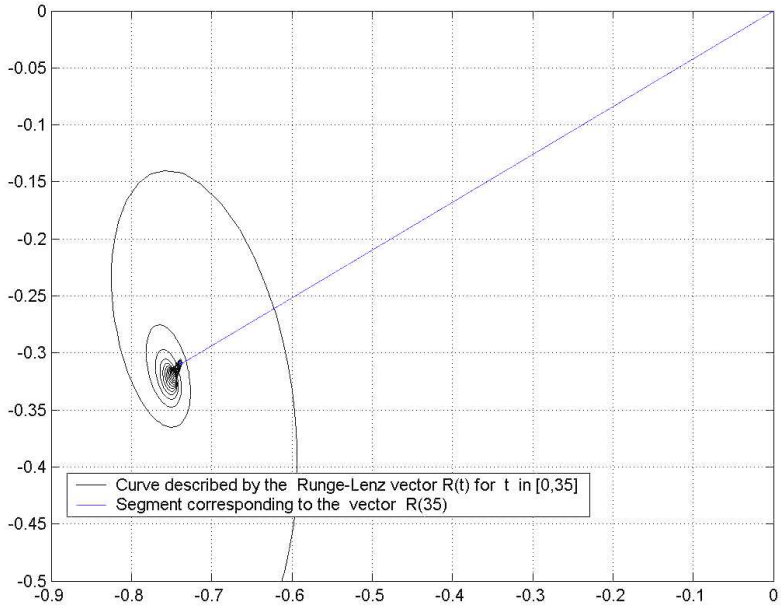

Figure 2: Plot of the evolution in time of the eccentricity vector $R(t)$ corresponding to the solution in Figure 1. As t varies in the interval $[0, 35]$ the vector describes the black curve. It is apparent its tendency to stabilize. To highlight its final value $R(35)$ is represented with a line segment starting at $(0, 0)$.

velocity which tends to zero and along a limit direction (this last property was also presented in [3]). This is in sharp contrast with the results obtained in [14] for the non rectilinear motions of the linear drag (no collision in finite time, energy which goes to $-\infty$ as $t \to +\infty$) and in corollaries 3.1 and 3.3 of this paper (motions with $|I| < 1$ tend to the singularity along spirals which shrink exponentially with time. In addition these motions wind around the origin with angular velocity that increases exponentially with time).

Although the linear drag is not relevant for artificial satellites dynamics, since in this setting it is assumed a velocity square law in drag acceleration together with an atmosphere density exponentially decreasing with altitude (see [2]), we would like to mention that the formulation of Corollary 3.3 was inspired by the data of the orbital parameters collected from the Sputnik 1 mission [18, page 105]. In particular, these data showed that the orbital period was decreasing as the satellite was getting closer to the Earth. Quoting [18] "..a fact which may appear paradoxical at a first glance: the atmosphere

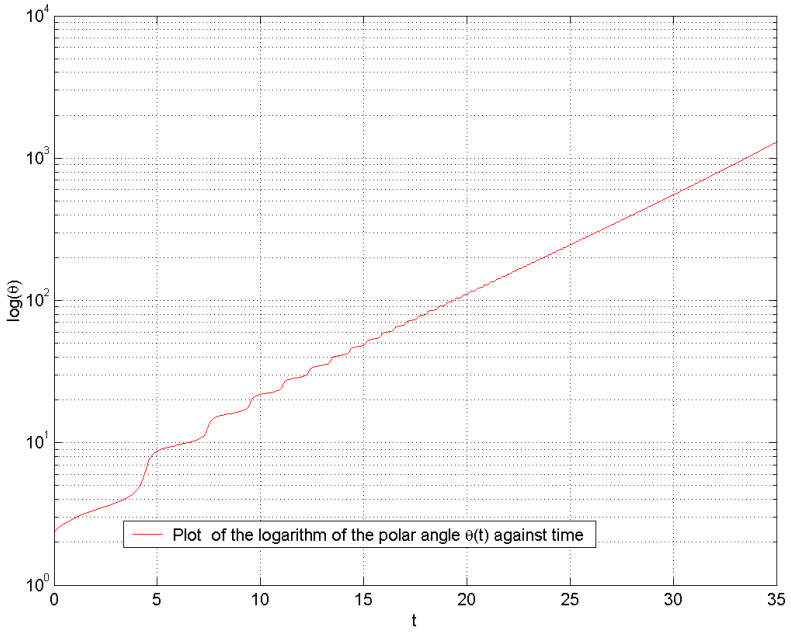

Figure 3: For the same solution as in the previous figures, the plot of the evolution in time of $\log(\theta(t))$ illustrates the exponential growth of $\theta(t)$ corresponding to (44).

impedes the motion of the satellite, yet the latter circuits the Earth faster and faster!" To obtain a result analogous to Corollary 3.3 for a physically realistic drag of the form $e^{-\alpha|x|}|\dot{x}|\dot{x}$, $\alpha > 0$, would allow to give a theoretical explanation of this phenomenon.

We remark that the results presented here for the linear drag follow quite directly from the existence of a continuous first integral, obtained as asymptotic Runge-Lenz vector. The problem of its actual degree of smoothness seems difficult, as does the problem of its existence for a more general drag of the form $D(x, \dot{x}) = D(|x|)$, with $A \leq D(|x|) \leq B$.

Finally, we think that a qualitative theory of the Kepler problem with drag should aim at an understanding of the qualitative differences in the global dynamics for different classes of drags. We intend to continue our efforts in this direction.

5 Appendix

Proof of Lemma 2.2. To understand the need for all the subtleties involved in the proof it is convenient to start with a special case. By now we impose the additional assumption $K \cap M_0 = \emptyset$ with $M_0 = \{(x, v) \in \Omega : \ x \wedge v = 0\}$. In this case we know that the energy $E(t; x_0, v_0)$ tends decreasingly to $-\infty$ as $t \to +\infty$ for each $(x_0, v_0) \in K$. By continuous dependence we can find an instant $t_* = t_*(x_0, v_0) > 0$ and an open neighbourhood $\mathcal{U} = \mathcal{U}(x_0, v_0)$ such that

$$E(t_*; x_0, v_0) < -\frac{1}{2} \ \text{ if } \ (x_0, v_0) \in \mathcal{U}. \tag{53}$$

Next we use the compactness of K to find a finite covering of the type $\{\mathcal{U}(x_0^{(i)}, v_0^{(i)})\}_{1 \le i \le n}$. If we define

$$\tau = \max\{t_*(x_0^{(i)}, v_0^{(i)}) : \ 1 \le i \le n\},$$

we obtain

$$E(\tau; x_0, v_0) < -\frac{1}{2} \ \text{ for each } \ (x_0, v_0) \in K. \tag{54}$$

Then

$$|x(t; x_0, v_0)| < \frac{1}{|E(t; x_0, v_0)|} < 2 \ \text{ if } t \ge \tau. \tag{55}$$

By continuous dependence we know that the number

$$\hat{m}_K = \max\{|x(t; x_0, v_0)| : \ t \in [0, \tau], (x_0, v_0) \in K\} \tag{56}$$

is finite. The claim holds with $m_K = \max\{2, \hat{m}_K\}$.

The previous argument cannot be employed when $K \cap M_0 \neq \emptyset$. In this case some solutions are only defined in the future on an interval $[0, \omega[$ with $\omega < \infty$ and the limit of the energy as $t \to \omega$ can be any number (see again [14]). However, if we replace classical solutions on M_0 by bouncing solutions (obtained by gluing collision-ejection solutions in a sequence, adjacent ejection and collision occurring with the same energy) then they will be defined for all future times and the energy will eventually become negative. This observation will be made rigorous via the Levi-Civita regularization that was presented in [14]. We recall that, after the natural identification of $x = (x_1, x_2)$ with the complex number $x_1 + ix_2$, the Levi-Civita regularization is defined by the change of variables

$$x = w^2, \ ds = \frac{dt}{|x|}. \tag{57}$$

Using this regularization equation (1) is transformed into the polynomial system of ODEs in the new time s

$$w' = v, \quad v' = \frac{Ew}{2} - \epsilon|w|^2 v, \quad E' = -2\epsilon(E|w|^2 + 1). \tag{58}$$

This system has to be considered on the invariant manifold

$$\mathcal{M} = \{(w, v, E) \in \mathbb{C}^2 \times \mathbb{R} : \ E|w|^2 + 1 - 2|v|^2 = 0\}, \tag{59}$$

which contains all the physically meaningful solutions. Let $(w(s), v(s), E(s))$ be a solution lying on $\mathcal{M}$. We claim that this solution is defined on $[0, \infty[$ and that the energy $E(s)$ eventually becomes negative. Assume that $[0, \sigma[$ is the maximal interval to the right. From the equation defining the manifold $\mathcal{M}$ we deduce that

$$|w'(s)| = \sqrt{\frac{1 + E(s)|w(s)|^2}{2}}.$$

This leads to the differential inequality for $|w(s)|$,

$$\frac{d}{ds}|w(s)| \leq |w'(s)| \leq \sqrt{\frac{1 + E(0)|w(s)|^2}{2}}, \tag{60}$$

and a standard continuation argument shows that $\sigma = \infty$. To prove that the energy is eventually negative we reason by contradiction and assume that $E(s)$ has a limit $E_\infty \geq 0$ as $s \to +\infty$. Then $E(s) > 0$ for each $s > 0$ and

$$E(s) = E(0) - 2\epsilon \int_0^s (E(\xi)|w(\xi)|^2 + 1) d\xi \leq E(0) - 2\epsilon s \to -\infty, \tag{61}$$

a contradiction with $E_\infty \geq 0$. We are ready to present the complete proof of the lemma. Given $(x_0, v_0) \in K$ we can produce two initial conditions $(w_0, \hat{v}_0, E_0)$ for the regularized system (58)-(59). After identifying x_0 and v_0 with complex numbers, w_0 will be a square root of x_0, $\hat{v}_0 = \frac{|x_0| v_0}{2 w_0}$ and $E_0 = \frac{1}{2}|v_0|^2 - \frac{1}{|x_0|}$. We observe that the triplets $(w_0, \hat{v}_0, E_0)$ lie on a compact subset $\mathcal{K}$ of $\mathcal{M}$. The same type of compactness argument as in the previous case shows the existence of a number s_* depending only on $\mathcal{K}$ (and hence on K) such that

$$E(s; w_0, \hat{v}_0, E_0) < -\frac{1}{2} \ \text{ if } \ s \geq s_* \text{ and } (w_0, \hat{v}_0, E_0) \in \mathcal{K}. \tag{62}$$

Define

$$\hat{m}_{\mathcal{K}} = \max\{|w(s; w_0, \hat{v}_0, E_0)|^2 : \ s \in [0, s_*], (w_0, \hat{v}_0, E_0) \in \mathcal{K}\} < \infty. \tag{63}$$

Going back to the original variables and time we deduce that

$$|x(t;x_0,v_0)| \leq \hat{m}_{\mathcal{K}} \text{ if } 0 \leq t \leq t_* \text{ and } |x(t;x_0,v_0)| \leq 2 \text{ if } t \geq t_*, \tag{64}$$

where

$$t_* = \int_0^{s_*} |w(s;w_0,\hat{v}_0,E_0)|^2 ds \text{ for each } (w_0,\hat{v}_0,E_0) \in \mathcal{K}. \tag{65}$$

The instant t_* will be different for each initial condition but this creates no trouble because the number $m_K = \max\{2, \hat{m}_{\mathcal{K}}\}$ only depends on K. ■

References

[1] Ai, Chong, Effect of tidal dissipation on the motion of celestial bodies, Thesis (Ph.D.), The Pennsylvania State University, (2012), 51 pp. ISBN: 978-1303-05123-4

[2] Brouwer D. and Hori G. I., Theoretical evaluation of atmospheric drag effects in the motion of an artificial satellite., *Astron. J.* (1961), 66, 193–225

[3] Breiter, S. and Jackson, A., Unified analytical solutions to two-body problems with drag, *Mon. Not. R. Astron. Soc*, (1998), 299, 237–243.

[4] Celletti, A., Stability and Chaos in Celestial Mechanics, Springer Verlag, Berlin (2010) (published in association with Praxis Publ. Ltd. Chichester).

[5] Calleja, R.C, Celletti, A., De la Llave R., A KAM theory for conformally symplectic systems: Efficient algorithms and their validation, *J. Differential Equations*, (2013), 255, 978–1049.

[6] Corne, J.L. and Rouche, N., Attractivity of closed sets proved by using a family of Lyapunov functions, *J. Differential Equations*, (1973), 13, 231–246.

[7] Danby, J. M. A., Fundamentals of celestial mechanics, The Macmillan Company, New York, (1962),

[8] Diacu, F., Two body problems with drag or thrust: qualitative results, *Celest. Mech. Dyn. Astr.*, (1999), 75: 1–15.

[9] V.M. Gorringe and Leach, P. G. L. , Hamilton-like vectors for a class of Kepler problem with a force proportional to the velocity, *Celestial Mechanics,* (1988), 41: 125–130.

[10] Goldstein, H., Classical Mechanics, Addison-Wesley (1980).

[11] V.M. Gorringe and Leach, P. G. L. , Hamilton-like vectors for a class of Kepler problem with a force proportional to the velocity, *Celestial Mechanics,* (1988), 41: 125–130.

[12] Jacobi, C. G. J., Jacobi's lectures on dynamics, *Texts and Readings in Mathematics*, 51, Hindustan Book Agency, New Delhi, (2009)

[13] Leach, P. G. L. , The first integrals and orbit equation for the Kepler problem with drag, *J. Phys. A,* (1987), 20: 1997–2002.

[14] Margheri, A., Ortega, R., Rebelo, C., Dynamics of Kepler problem with linear drag, *Celestial Mech. Dynam. Astronom.*, (2014), 120: 19–38.

[15] Mavraganis, A. G. and Michalakis, D. G., The two-body problem with drag and radiation pressure,*Celestial Mech. Dynam. Astronom.*, (1994): 4, 393–403.

[16] Moser, J., Integrals via asymptotics; the Störmer problem, *unpublished*, (1963)

http://www.math.harvard.edu/˜knill/diplom/lit/Moser1963.pdf

[17] Moser, J., Zehnder, E. J. Notes on Dynamical Systems, (2005),12, Courant Lecture Notes, AMS.

[18] Ryabov, Y., Yankovsky, G., An Elementary Survey of Celestial Mechanics, (1961) Dover Publications, Inc. New York.